Exp Fluids (2011) 51:835–851
DOI 10.1007/s00348-011-1102-6

RESEARCH ARTICLE

# Characterization of the wind loads and flow fields around a gable-roof building model in tornado-like winds

**Hui Hu · Zifeng Yang · Partha Sarkar · Fred Haan**

Received: 2 January 2011 / Revised: 9 April 2011 / Accepted: 16 April 2011 / Published online: 1 May 2011


**Abstract** An experimental study was conducted to quantify the characteristics of a tornado-like vortex and to reveal the dynamics of the flow-structure interactions between a low-rise, gable-roof building model and swirling, turbulent tornado-like winds. The experimental work was conducted by using a large-scale tornado simulator located in the Aerospace Engineering Department of Iowa State University. In addition to measuring the pressure distributions and resultant wind loads acting on the building model, a digital Particle Image Velocimetry system was used to conduct detailed flow field measurements to quantify the evolution of the unsteady vortices and turbulent flow structures around the gable-roof building model in tornado-like winds. The effects of important parameters, such as the distance between the centers of the tornado-like vortex and the test model and the orientation angles of the building model related to the tornado-like vortex, on the evolutions of the wake vortices and turbulent flow structures around the gable-roof building model as well as the wind loads induced by the tornado-like vortex were assessed quantitatively. The detailed flow field measurements were correlated with the surface pressure and wind load measurements to elucidate the underlying physics to gain further insight into flow-structure interactions between the gable-roof building model and tornado-like winds in order to provide more accurate prediction of wind damage potential to built structures.

H. Hu (✉) · Z. Yang · P. Sarkar · F. Haan
Department of Aerospace Engineering, Iowa State University,
2271 Howe Hall, Room 1200, Ames, IA 50011, USA
e-mail: huhui@iastate.edu

*Present Address:*
F. Haan
Department of Mechanical Engineering,
Rose-Hulman Institute of Technology,
Terre Haute, IN 47803-3999, USA

## 1 Introduction

Tornadoes are powerful columns of winds spiraling around centers of low atmospheric pressure, which are often (but not always) visible as funnel clouds. Tornadoes are considered as nature's most violent storms, which can produce the highest natural wind speeds on earth, i.e., with the maximum wind speed up to 400 mph (Grazulis 1993). Large-scale damage and heavy loss of life caused by intense tornado outbreaks in populated areas have been reported frequently in the past years (Brooks and Doswell 2001; Speheger et al. 2002; Doswell et al. 2006; Forbes 2006). Some of the well-known tornadoes include the Tri-State tornado of March 18, 1925, killed 695 people and the Natchez, Mississippi tornado of May 7, 1840, claimed 317 lives. The 1965 Palm Sunday tornado outbreak was the second deadliest of the twentieth century, killing 258 people and injuring 3,148. The 1999 Oklahoma tornado outbreak that lasted from May 3 to May 6, 1999, stands as the costliest tornado in United States history having destroyed nearly 11,000 buildings and causing over $1.9 billion in damage.

According to Wind Hazard Reduction Coalition statistics, an average of 800–1,000 tornados occurs each year in the United States alone. Statistics also show that almost 90% of all recorded tornados are rated F2 or less on the Fujita Scale, i.e., they involve wind speeds less than 160 mph (Bluestein and Golden 1993; Womble et al. 2009). It has been suggested that it is economically feasible to design built structures such as commercial buildings, bridges, hospitals, power plants, and airports to resist F2 or

even stronger tornados. Any such design work, however, requires a keen understanding of the nature of tornadoes and accurate estimations about the tornado-induced wind loads and wind field information around built civil structures due to the presence of tornados.

With the consideration of buildings as surface-mounted obstacles, extensive experimental and numerical studies have been carried out in recently years to investigate the flow-structure interactions between building models and turbulent winds as well as the resultant wind loads acting on the building models (Cermak 1975; Castro and Robins 1977; Hunt et al. 1978; Martinuzzi and Tropea 1993; Shah and Ferziger 1997; Krajnovic and Davidson 1999; Kim et al. 2003; Yakhot et al. 2006; Yang et al. 2011). Besides the studies using prismatic obstacles to represent cube-shaped buildings, several studies have also been conducted to consider more realistic low-rise residential building models with various roof shapes (Holmes 1993; Kanda and Maruta 1993; Peterka et al. 1998; Stathopoulos et al. 2001, and Sousa 2002; Sousa and Pereira 2004; Liu et al. 2009) to quantify the effects of the gable-roof shape on the wake flow behaviors as well as the resultant wind loads acting on the low-rise gable-roof building models.

While a great deal has been uncovered about the dynamics of the flow-structures interactions between the building models and incoming turbulent winds as well as the resultant wind loads by those studies, most of the previous studies were conducted with the building models placed in straight-line boundary layer winds. It is well known that tornadoes are strong vortices with significant tangential component, radial inflow/outflow, and vertical updraft/downdraft. Tornado-induced wind loads and the dynamics of the flow-structure interaction between the buildings and the swirling tornado winds may be quite different from those in straight-line boundary-layer flows (Chang 1971; Ward 1972; Markowski et al. 2002). Surprisingly, although strong tornadoes are well-known natural hazards, very few studies specifically address the dynamics of the flow-structure interactions between building models and tornado-like vortices and the wind loads induced by tornado-like winds. While some numerical studies have been made in recent years on the flow characteristics of tornado-like winds (Lee and Wilhelmson 1997a, b; Schecter et al. 2008; Natarajan 2011), Jischke and Light (1983) and Bienkiewicz and Dudhia (1993) conducted comparative studies to measure the wind loads and surface pressure on small building models in swirling, tornado-like winds, and straight-line winds. They found that the wind loads acting on the test models are significantly higher (3–5 times) in swirling, tornado-like winds. The surface pressure distributions on the tested building models in tornado-like winds are also quite different compared with those in straight-line winds. The findings highlights that it is incorrect, at least incomplete, to use a conventional straight-line boundary layer wind tunnel running with maximum tornado wind speed to estimate the tornado-induced wind loads on built structures. It should also be noted that almost all the previous work on building models in tornado-like winds were conducted by measuring wind loads and/or surface pressure distributions only (Nolan and Farrell 1999; Sengupta et al. 2008; Mishra et al. 2008a, b; Haan et al. 2010), no study has ever been conducted so far to provide detailed flow field measurements to quantify the characteristics of tornado-like vortices and to reveal the dynamics of the flow-structure interactions between building models and swirling tornado-like winds.

While tornado-induced damages have been reported for both low-rise and high-rise buildings (Yang et al. 2011), the patterns of the tornado-induced damages to high-rise buildings and low-rise buildings are quite different in nature. Tornado-induced damages to low-rise residential buildings are usually associated with structural or large component failures such as complete collapse or roofs being torn-off, while tornado damage to high-rise buildings are generally associated with building envelope failures with no or little structural damage. As a result, tornado-induced damages to low-rise gable-roof buildings are more fatal and more commonly seen in the aftermaths of intense tornadoes.

In the present study, a comprehensive study was conducted to quantify the characteristics of a tornado-like vortex and to reveal the dynamics of the flow-structure interactions between a low-rise, gable-roof building model and swirling, turbulent tornado-like winds. The effects of important parameters, such as the distance between the centers of the tornado-like vortex and the test model and the orientation angles of the building model related to the tornado-like vortex, on the evolutions of the wake vortices and turbulent flow structures around the gable-roof building model as well as the wind loads induced by the tornado-like vortex were assessed quantitatively. While pressure taps and a high-sensitivity load cell were used to map the pressure distributions around the building model and to measure the wind loads (forces and moments) acting on the test model induced by tornado-like winds, a digital Particle Image Velocimetry (PIV) system was used to conduct detailed flow field measurements to quantify the evolution of the unsteady vortices and turbulent flow structures around the gable-roof building model in tornado-like winds. To our best knowledge, this is the first effort of its kind. The detailed flow field measurements were correlated with the wind load measurements to elucidate the underlying physics to gain further insight into flow-structure interactions between the low-rise gable-roof building model and tornado-like winds in order to provide more accurate prediction of wind damage potential to built

structures. It should be noted that our first report on this topic was made in a short note (Yang et al. 2010) with some preliminary measurement results. The present work adds much more detailed measurement results, extensive discussions and considerable analysis to elucidate the underlying physics, which is far beyond the scope of the short note of Yang et al. (2010).

## 2 Experimental setup

### 2.1 ISU tornado simulator

The experimental study was conducted by using a large-scale tornado simulator located in the Aerospace Engineering Department of Iowa State University (ISU). Figure 1 shows the schematic and photo depicting the flow circuit and dimensions of the ISU tornado simulator. A circular duct of 5.49 m in diameter and 3.35 m in height is suspended from a heavy duty overhead crane. A 1.83 m diameter fan (maximum flow rate is 59.0 $m^3/s$, 125,000 cfm) is mounted concentrically inside the circular duct to generate a strong updraft. The flow from the fan is redirected downward in a 0.30-m-wide annular duct to simulate the rear flank downdraft (RFD) encirclement found in natural tornados (Chang 1971; Davies-Jones 1976). Swirling is imparted to the airflow in the duct by adjusting the angle of the vanes at the top of the tornado simulator. The downdraft air diverges upon hitting the ground with most of the flow moving inward toward the fan. The fan updraft stretches the low-level vorticity into a tornado-like vortex. A unique feature of the ISU tornado simulator is that the tornado-like vortex can travel along the ground plane as the entire fan/downdraft-producing mechanism translates. This translation, along with the fact that there is a good clearance between the translating duct and the ground plane, allows a wide range of building models to be placed in the path of the tornado-like vortex for testing. More specifically, the ISU tornado simulator can generate a tornado-like vortex with a maximum diameter of 1.2 m and maximum tangential velocity of 14.5 m/s. The maximum swirl ratio (Church et al. 1977) achieved is 1.14, and the translation speed of the tornado-like vortex can reach up to 0.8 m/s. The vortex height can vary from 1.2 m to 2.4 m by adjusting the ground plane upward or downward. Further information about the design, construction, and performance of the ISU tornado simulator as well as the quantitative comparisons of the tornado-like vortex generated by using the ISU tornado simulator with the tornados found in nature can be found at Haan et al. (2008).

For the measurement results given in the present study, the ground floor was fixed at 0.457 m below the exit of the outer duct and the fan speed was fixed at 20 Hz (1/3rd of the full speed). The radius of the tornado-like vortex core, $R_O$, measured at the 30 mm above the ground plane (i.e., the horizontal plane passing the eave of the gable-roof building model) was found to be about 0.16 m (i.e., $R_O \approx 0.16$ m), at where the maximum tangential speed (i.e., $V_O = 10.0$ m/s) was observed. The corresponding (radial) Reynolds number of the tornado-like vortex is about 100,000. In the present study, the swirl ratio of the tornado-like vortex, which was calculated according to the expression of $S = \pi V_O R_O^2/Q$ with $Q$ being the flow rate through the fan, was about 0.1. The aspect ratio, which is defined as the ratio between the height and the radius of the tornado-like vortex, was about 4.0. According to Haan et al. (2008), with the parameter setting described above, the vortex generated by ISU tornado simulator would be a single-cell-typed tornado-like vortex, which is also confirmed from the PIV measurement results to be discussed later. It should be noted that, while the effects of the translation motion of the tornado-like vortex on the wind loads on buildings can be investigated by using ISU tornado

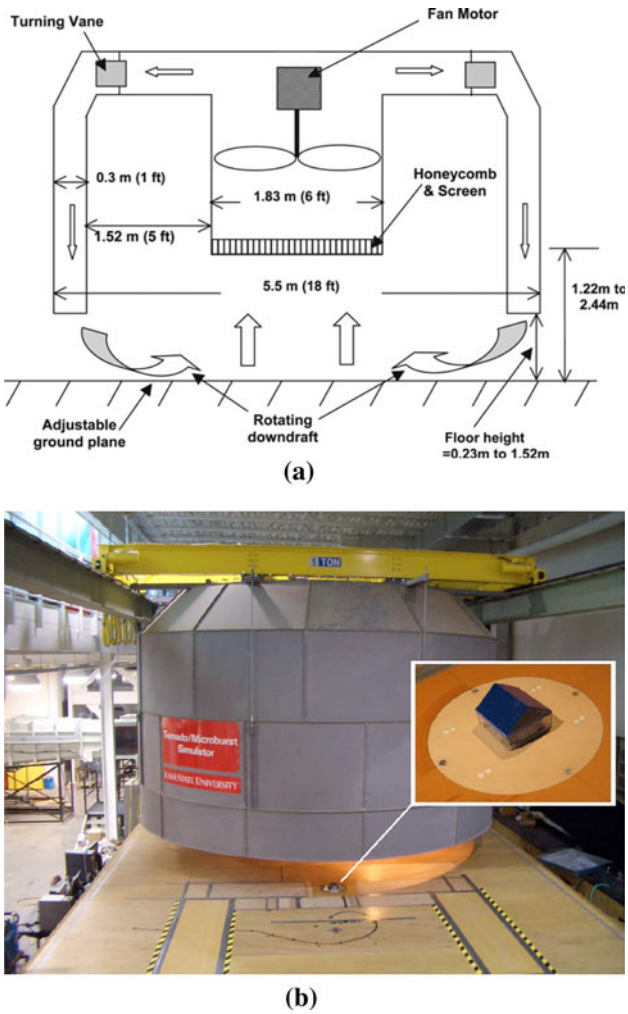


**Fig. 1** Schematic and photo of the ISU tornado simulator. **a** Schematic diagram. **b** Photo of the ISU tornado simulator

simulator, all measurement results given in the present study were made under the condition that ISU tornado simulator was fixed at a point during the measurement (i.e., without translation motion).

## 2.2 The gable-roof building model

Figure 2a shows schematic of the low-rise, gable-roof building model used in the present study. The test model has a base of 90 mm × 90 mm in cross section, an eave height of 30 mm, and gable-roof angle of about 35°. It has been found that tornadoes can occur in a wide range of sizes with the core radius varying from a few meters to kilometers (Bluestein and Golden 1993). By setting a length scale of 1:200, the research work presented here will simulate the flow-structure interactions of a tornado with the core diameter about 65 meters, i.e., approximately the size of the Dallas tornado of April 2, 1957 (Haan et al. 2010), and a low-rise gable-roof building of 18 m × 18 m in cross section and an eave height of 6.0 m.

In the present study, three building models with identical geometric shape and dimension were made for the experimental investigations. The first one was made of thin plastic plates with 89 pressure taps on the surface in order to measure the surface pressure distributions around the house model. As shown in Fig. 2b, the roof contains a total of 43 pressure taps with 24 taps on the side first to be struck with tangential winds and 19 pressure taps on the opposite side of the roof. The building walls contain nine pressure taps on each side, and the two triangular gable end sections contain five taps each. The pressure taps were connected to high-speed electronic pressure scanners (Scanivalve-ZOC33/64Px) with the pressure data sampled at the rate of 500 Hz for 30 s for each tested case.

The second model was constructed as a single unit using rapid prototyping technique with an aluminum rod through

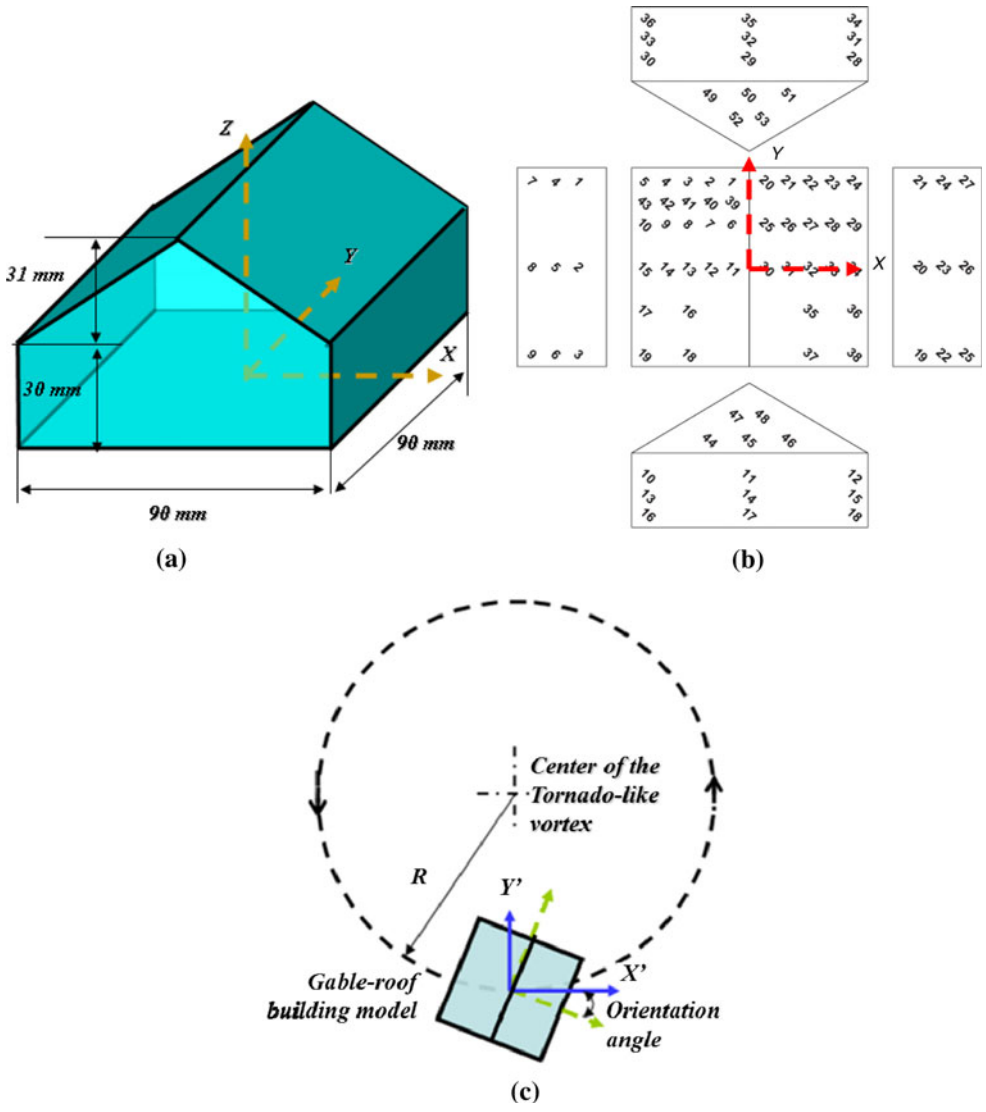


**Fig. 2** The gable-roof building model and its position and orientation related to the tornado-like vortex. **a** The gable-roof building model. **b** Exploded view with pressure taps. **c** Position and orientation of the test building model related to the tornado-like vortex

the center as the main structural support. This rod was connected through a hole in the ground plane to a high-sensitivity force-moment sensor (JR3, model 30E12A-I40) to measure the resultant wind load (both force and moment) induced by the tornado-like winds. The JR3 load cell is composed of foil strain gage bridges, which are capable of measuring the forces on three orthogonal axes, and the moment (torque) about each axis. The precision of the force-moment sensor cell for force measurements is ±0.25% of the full range (40 N). In the present study, the aerodynamic force and moment coefficients were defined by using the equations:

$$CF_X = \frac{F_X}{\frac{1}{2}\rho V_O^2 A}; CF_Y = \frac{F_Y}{\frac{1}{2}\rho V_O^2 A}; CF_Z = \frac{F_Z}{\frac{1}{2}\rho V_O^2 A}$$

$$CM_X = \frac{M_X}{\frac{1}{2}\rho V_O^2 AH}; CM_Y = \frac{M_Y}{\frac{1}{2}\rho V_O^2 AH}; CM_Z = \frac{M_Z}{\frac{1}{2}\rho V_O^2 AH},$$

where $\rho$ is the air density, $V_O$ is the wind speed at the outer boundary of the tornado-like vortex core, $A$ is the projected area of the gable-roof building model along the Y-direction as shown in Fig. 2a, $H$ is the spanwise length of the building model along the Y-direction.

It should be noted that the projected areas of the building model along each axis directions were usually used to define the corresponding force and moment coefficients in previous studies (Uematsu et al. 2007; Haan et al. 2010). In the present study, the same area, i.e., the projected area along the Y-axis direction (i.e., the direction normal to the tangential velocity in the tornado-like winds), was used to normalize the wind loads acting on the gable-roof building model induced by tornado-like winds in all the directions in order to make direct comparisons of the magnitude of the aerodynamic forces and moments along X, Y, and Z directions.

The third test model one was made of transparent Plexiglas, which was used for PIV measurements to quantify the evolution of the unsteady vortex and turbulent flow structures around the gable-roof building model. For the PIV measurements, the flow was seeded with $\sim$1 μm oil droplets by using a droplet generator. Illumination was provided by a double-pulsed Nd:YAG laser (NewWave Gemini 200) adjusted on the second harmonic and emitting two pulses of 200 mJ at the wavelength of 532 nm with a repetition rate of 10 Hz. The laser beam was shaped to a sheet by a set of mirrors with spherical and cylindrical lenses. The thickness of the laser sheet in the measurement region was about 1.0 mm. A high resolution 12-bit CCD camera (Pixelfly, CookeCorp) was used for PIV image acquisition with the axis of the camera perpendicular to the laser sheet. The CCD camera and the double-pulsed Nd:YAG lasers were connected to a workstation (host computer) via a Digital Delay Generator (Berkeley Nucleonics, Model 565), which controlled the timing of the laser illumination and the image acquisition. Instantaneous PIV velocity vectors were obtained by a frame to frame cross-correlation technique involving successive frames of patterns of particle images in an interrogation window of 32 × 32 pixels. An effective overlap of 50% of the interrogation windows was employed in PIV image processing. The time-averaged velocity ($U$, $V$) distributions were obtained from a cinema sequence of 500 frames of measured instantaneous velocity fields. The measurement uncertainty level for the velocity vectors was estimated to be within 2.0%.

In the present study, the effects of important parameters, such as the distance between the centers of the tornado-like vortex and the gable-roof building model and the orientation angles of the building model related to the tornado-like vortex, on the evolutions of the wake vortices and turbulent flow structures around the gable-roof building model as well as the wind loads induced by the tornado-like vortex were assessed quantitatively. Figure 2c shows the position and orientation of gable-roof building model in relation to the tornado-like vortex, where $R$ is defined as the distance between the centers of the tornado-like vortex and the test building model, and OA is the orientation angle of the building model.

## 3 Results and discussions

### 3.1 The characteristics of a tornado-like vortex

In the present study, PIV measurements were conducted to quantify the characteristics of the tornado-like vortex generated by the ISU tornado simulator before the gable-roof building models were mounted on the test ground plane. Figure 3 shows the typical instantaneous and time-averaged PIV measurement results (i.e., velocity distributions and the corresponding streamlines) of the tornado-like vortex in the horizontal planes at different elevations above the test ground plate. It can be seen clearly that, with the experimental controlling parameters described above, the vortex generated by the ISU tornado simulator was a single-cell-typed tornado-like vortex, which confirmed the observations of Haan et al. (2008) quantitatively. The time sequences of the instantaneous PIV measurement results revealed clearly that the tornado-like vortex was highly turbulent with the size, shape, and the position of its vortex center varying significantly from one frame to another. The center of the tornado-like vortex was tracked based on the time-sequence of the instantaneous PIV measurements to investigate the wandering behavior of the tornado-like vortex. Figure 4 shows the moving trajectory of the center of the tornado-like vortex based on 500 frames of instantaneous PIV measurement results in the horizontal plane of $Z/R_O \approx 0.10$ (i.e., the horizontal plane crossing the middle

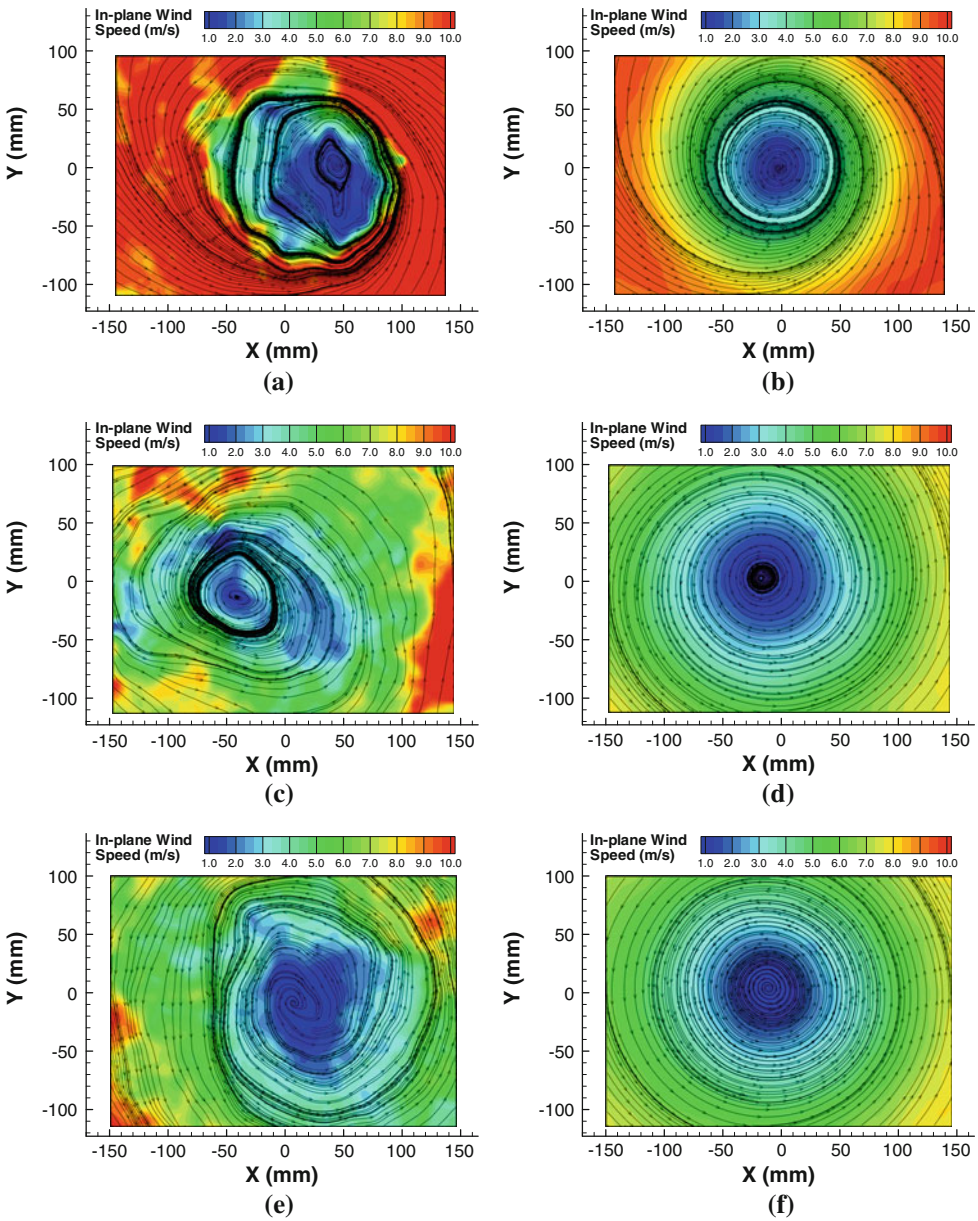


**Fig. 3** Typical instantaneous and ensemble-averaged PIV measurement result of the tornado-like vortex in the horizontal planes at different elevations. **a** Instantaneous results in $Z/R_O \approx 0.10$ plane. **b** Ensemble-averaged results in $Z/R_O \approx 0.10$ plane. **c** Instantaneous results in $Z/R_O \approx 0.40$ plane. **d** Ensemble-averaged results in $Z/R_O \approx 0.40$ plane. **e** instantaneous results in $Z/R_O \approx 0.70$ plane. **f** Ensemble-averaged results in $Z/R_O \approx 0.70$ plane

plane of the vertical walls of the gable-roof building model). It can be seen clearly that, while the instantaneous center of the tornado-like vortex was found to be scattering around the time-averaged center of the vortex randomly, the wandering of the tornado-like vortex were found to be almost symmetrical to its time-averaged center with the maximum wandering amplitude about 0.6 times of the vortex radius. Further data reduction reveals that the probability density function (pdf) of the instantaneous location of the tornado-like vortex center during the wandering movement can be represented well by using a Gaussian function with the standard deviation $\sigma_x \approx \sigma_y \approx 0.3R_O$.

While the instantaneous PIV measurement results reveal clearly that the tornado-like vortex was highly turbulent with its center wandering around randomly, a well-defined flow pattern in the form of a single counter-clockwise vortex structure can be identified clearly from the time-averaged PIV measurement results in the horizontal planes at different elevations. As visualized clearly in the plots shown in Fig. 3b, d, f, the streamlines of the time-averaged flow field in the core region of the tornado-like vortex were found to be concentric circles. While the magnitude of the flow velocity was found to increase almost linearly with the increasing radial distance away from the vortex center (the measured velocity profile is given in Fig. 6), the radial components of the flow velocity vectors in the core region of the tornado-like vortex were found to be very small, which is almost negligible compared with the tangential components. Such measurement results indicate that the flow in the core region of the tornado-like vortex would be

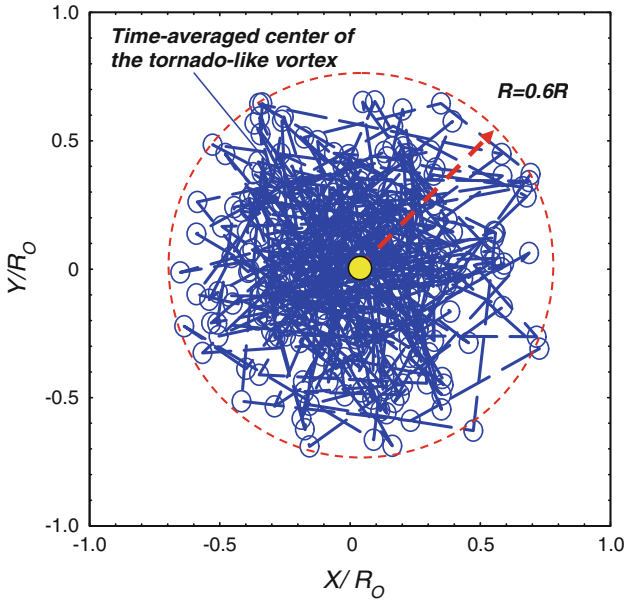


**Fig. 4** Wandering of the tornado-like vortex in the horizontal plane of $Z/R_O \approx 0.10$

very much like that of a potential vortex with the flow velocity vectors being mainly tangential. For the comparisons of the time-averaged flow field at different elevations, it can be seen clearly in Fig. 3 that the size of the vortex core (i.e., the region with concentric circular streamlines) was found to become bigger and bigger as the PIV measurement planes were moved further away from the ground plate. It indicates that the core region of the tornado-like vortex would become bigger and bigger as the height of the elevation increases, which agrees with the observations of the funnel-shaped cores of the tornadoes found in nature.

Figure 5 shows the time-averaged PIV measurement results in the horizontal plane of $Z/R_O \approx 0.10$ as the center of the tornado-like vortex was moved away from the center of the PIV measurement window (i.e., the location where the gable-roof building models will be mounted) along Y-axis direction. While the streamlines of the flow field in the core region of the tornado-like vortex were found to be concentric circles, the streamlines in the outer region of the tornado-like vortex revealed an interesting flow feature of the tornado-like wind, i.e., a spiral motion. As shown clearly in the plots, the flow velocity vectors in the region far away from the center of the tornado-like vortex were found to have significant radial components ($V_R$) compared with the tangential components ($V_\theta$). The PIV measurements revealed that a strong spiral flow would be generated in the outer region of the tornado-like vortex, which made the surrounding air streams flowing toward the core of the tornado-like vortex.

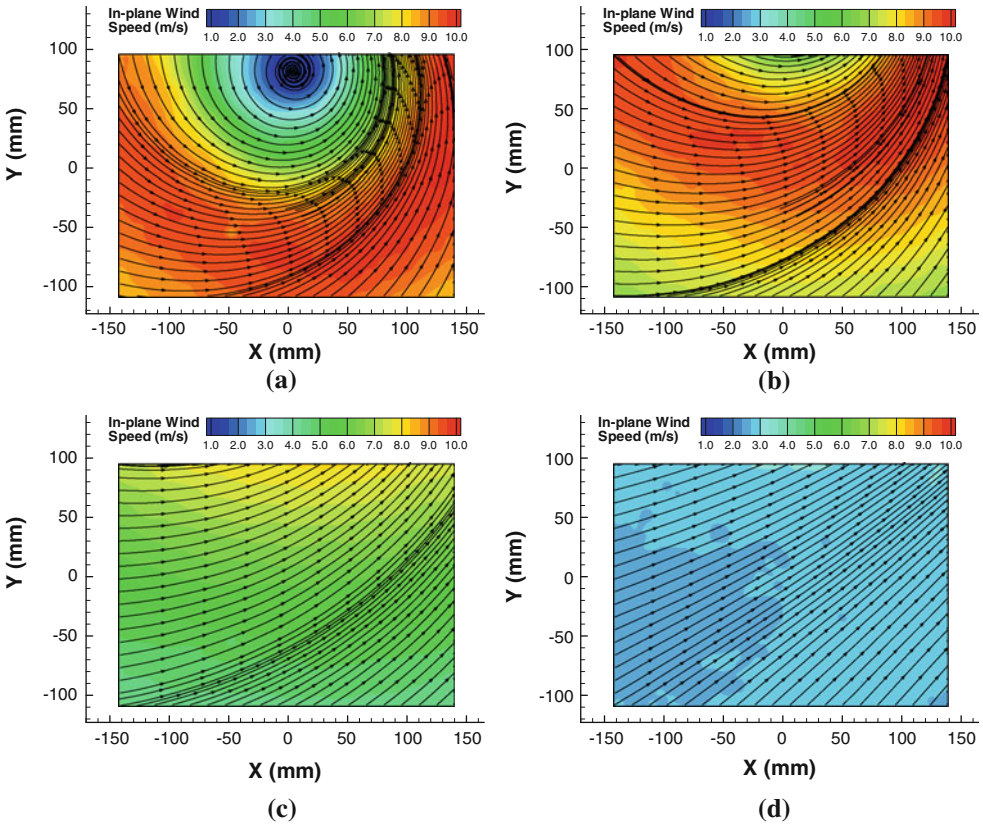


**Fig. 5** Ensemble-averaged PIV measurement results in the outer region of the tornado-like vortex ($Z/R_O \approx 0.10$). **a** $R/R_O \approx 0.50$. **b** $R/R_O \approx 1.0$. **c** $R/R_O \approx 2.0$. **d** $R/R_O \approx 4.5$

Figure 6 shows the measured velocity profiles of the tornado-like vortex in the terms of radial velocity ($V_R$) and tangential velocity ($V_\theta$) components compared with those of the field measurement data of two tornados (e.g., Spencer tornado of May 30, 1998, and Mulhall tornado of May 3, 1999) to demonstrate the similarity between the tornado-like vortex generated by using the ISU tornado simulator and the tornados found in nature. The field measurement data of the tornados used for the comparison were made available to ISU researchers by Mr. J. Wurman under a subcontract of a NSF-sponsored project, which were also published in Wurman and Alexander (2005). The field data were acquired using Doppler Radar on Wheels observations from the Spencer, South Dakota tornado of May 30, 1998, and the Mulhall, Oklahoma tornado of May 3, 1999. Figure 7 shows the profiles of the measured pressure on the test ground plane beneath the tornado-like vortex generated by the ISU tornado simulator compared with the field measurement data of the Manchester, SD tornado on June 24, 2003, provided by Mr. Tim Samaras under a subcontract of a NOAA-sponsored project (Samaras 2008). It can be seen clearly that, even though the tornado-like vortex generated by the ISU tornado simulator and the tornados found in nature have significant differences in their core diameters (e.g., 0.33 m for the tornado-like vortex generated by the ISU tornado simulator vs. approximately 400 m and 800 m for Spencer and Mulhall tornados, respectively), the overall flow structures of the vortices are quite similar.

The measured radial velocity profile given in Fig. 6 also reveal quantitatively that the radial components of flow velocity vectors in the core region of the tornado-like vortex (i.e. $R/R_O < 1.0$) are very small, which is almost negligible with respect to the other components. However, in the outside region of the tornado-like vortex ($R/R_O > 1.0$), the radial component of flow velocity was found to increase rapidly with the increasing radial distance away from the center of the tornado-like vortex.

The PIV measurement results described above revealed that the tornado-like vortex in each horizontal plane can be divided into two regions: an inner core region and an outer region. In the inner core region, air streams rotate concentrically with the wind speed increasing linearly with the increasing radial distance away from the rotation center. The flow inside the tornado-like vortex core rotates like a rigid column, i.e., the flow velocity vectors in the vortex core region were almost tangential with the radial components being almost negligible (i.e., $V_R \approx 0$). After reaching its peak value at the outer boundary of the tornado-like vortex core, wind speed was found to decrease gradually with the increasing distance away from the center of the tornado-like vortex in the outer region. The flow velocity vectors in the outer region of the tornado-like vortex have significant radial components flowing toward the center of the tornado-like vortex. As a result, a strong spiral motion is generated, which makes surrounding air streams flowing toward the core of the tornado-like vortex. The ground pressure measurement data shown in Fig. 7 revealed clearly that a significant low-pressure region was found to exist in the center of the tornado-like vortex, and the low pressure would recover gradually as the distance from the center of the tornado-like vortex increases.

Based on the PIV measurements in different vertical and horizontal planes, the 3-D flow structure of the tornado-like vortex was reconstructed, which is given in Fig. 8. A funnel-shaped profile was plotted in the figure to highlight

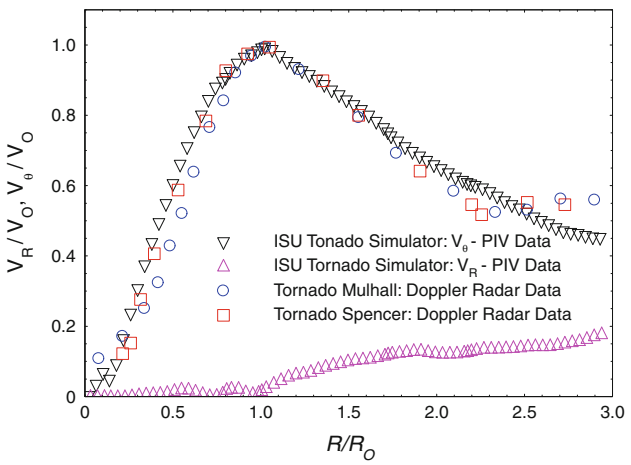


**Fig. 6** The tornado-like vortex versus Mulhall and Spencer tornadoes found in nature ($R_O$ is the radius of the tornado-like vortex core. $V_O$ is the wind speed at position of $R = R_O$. Doppler Radar Data were taken from Wurman and Alexander, 2005)

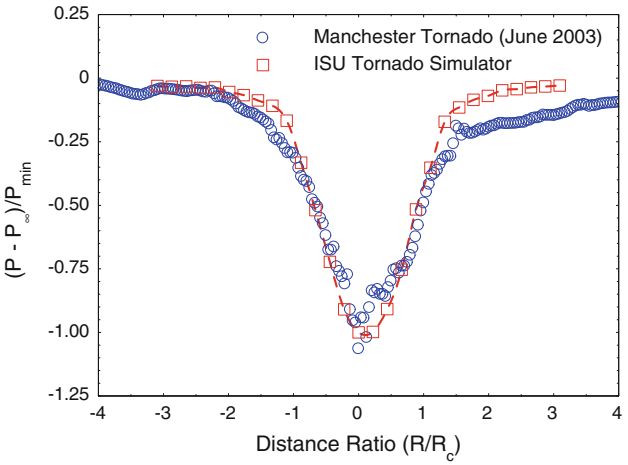


**Fig. 7** The profiles of the measured ground pressure of the tornado-like vortex generated by ISU tornado simulator versus the Manchester, SD tornado on June 24, 2003 (the field Data were taken by Tim Samaras; $P_{min}$ is the gauge pressure at the center of the tornado-like vortex; $P_\infty$ is the ambient pressure far away from the center of tornado-like vortex)

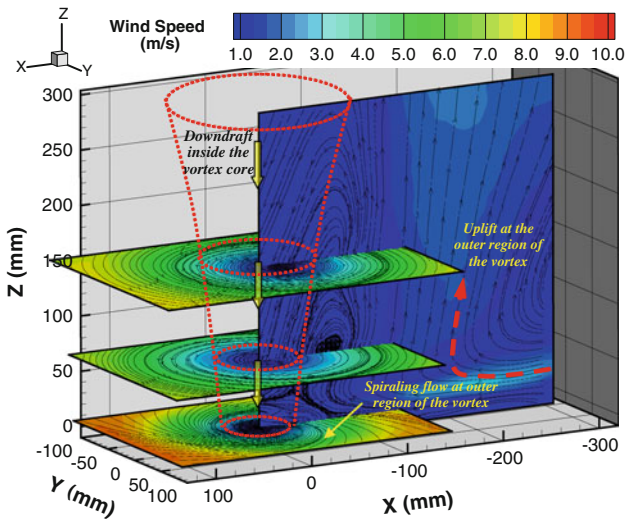


**Fig. 8** The flow characteristics of the tornado-like vortex

the size increase of the core region of the tornado-like vortex as the elevation level increases. The PIV measurement results in the vertical plane passing the time-averaged center of the tornado-like vortex were also shown in the plot. As revealed clearly from the PIV measurement results in the vertical plane, air streams near the ground far away from the center of the tornado-like vortex would flow toward the vortex core and turn upward abruptly before reaching the vortex core. It indicates that a radial and upward vertical flow would exist in the outer region of the tornado-like vortex, as expected. An interesting flow feature can be observed in the vortex core region, where flow is found to be a downdraft jet impinging onto the ground plate. As the downdraft jet approaching the ground plate in the vortex core, it would interact with the radial inflow streams from the outer region. As shown clearly in Fig. 8, a "recirculation bubble" structure was found to form near the ground between the upward outside flow streams and the downdraft jet in the core of the tornado-like vortex. The downdraft jet flow in the tornado-like vortex core revealed from the present PIV measurements was found to be well consistent to the findings of Wurman and Gill (2000), who conducted Doppler Radar measurements of the Dimmitt, Texas tornado on June 2, 1995, and found the downdraft jet flow in the tornado core penetrating up to 400 m above the ground level.

## 3.2 Flow-structure interactions between the building model and tornado-like winds

### *3.2.1 The effects of the distance between the centers of the tornado-like vortex and the test model*

Figure 9 shows the profiles of the measured wind loads (both force and moment coefficients) acting on the gable-roof building model as a function of the distance between the centers of the tornado-like vortex and the test model. During the experiments, the orientation angle (OA) of the building model related to the tornado-like vortex was set to 0.0 deg. (i.e., OA = 0.0 deg.). As revealed in Fig. 9, since the signs of the X, Y, and Z components of the measured aerodynamic forces are all positive, it indicates that the tornado-like wind would try to push the gable-roof building model tangentially; pull the building model toward the vortex core; and lift the building model up from the test ground, which are the most common damage patterns to the damaged low-rise buildings observed in the aftermath of intense tornado attacks in nature (Bluestein and Golden 1993).

The measured force coefficient profiles given in Fig. 9a also reveals clearly that all three components of the aerodynamic force acting on the gable-roof building model would increase with the increasing distance between the centers of the test model and the tornado-like vortex at first and then reach their peak values in the neighborhood of $R/R_O \approx 0.7$ for the uplift force (i.e., Z-component) and at $R/R_O \approx 1.0$ for the tangential pushing force (i.e., X-component) and inward pulling force (i.e., Y-component). As the building model was mounted in the outer region of the

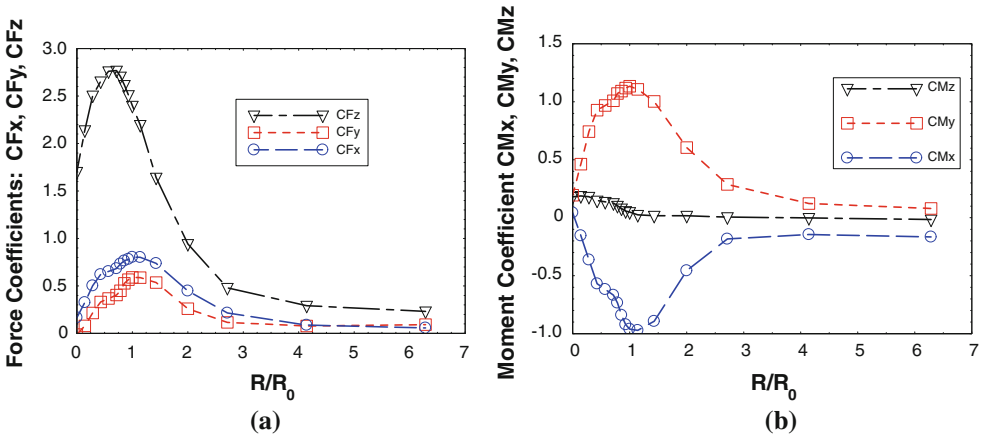


**Fig. 9** Measured wind loads versus the distance between the centers of the tornado-like vortex and the test model. **a**. Force coefficients. **b** Moment coefficients

tornado-like vortex core (i.e., $R/R_O > 1.0$), all three components of the aerodynamic force were found to decrease gradually with the increasing distance away from the center of the tornado-like vortex. The measurement results indicate that the building model would experience significant wind loads as it is mounted near the outer boundary of the tornado-like vortex core. Since the tangential components of the flow velocity vectors were found to be dominant in the core region of the tornado-like vortex, the X-component of the aerodynamic force, which is along the tangential direction of the flow streams approaching the building model, was found to be greater than the inward pushing force (i.e., Y-component). It should be noted that the Z-component of the aerodynamic force (i.e., the uplift force) was found to be the largest among the three components, which is more than three times stronger compared with the other two components. It is believed to be closely associated with the significant low pressure at the core region of the tornado-like vortex as shown in Fig. 7. The force measurement results revealed that the building model would experience significant roof uplift force as it was located near the core region of the tornado-like vortex. The finding is found to be consistent with the fact that the tornado-induced damage to low-rise, gable-roof buildings are often associated with torn-off roof.

The negative sign of the X-component of the measured moment coefficient, $CM_X$, indicates that the building model would likely bend toward the tornado-like vortex core due to the wind loads induced by tornado-like winds. The positive sign of the Y-component of the measured moment coefficient, $CM_Y$, indicates that the building model would bend toward tangential flow direction, as expected. Such collapsed patterns as expected from the above-mentioned features of $CM_X$ and $CM_Y$ are found to agree with those of the damaged buildings observed aftermath of tornado attacks in nature. The magnitude of the Z-component of the moment coefficient, $CM_Z$, was found to be much smaller than other two components, which is almost negligible. Similar to the measured force coefficients, the measured moment coefficients were also found to reach their peak values at the location of $R/R_O \approx 1.0$. The force and moment measurement results suggest that low-rise, gable-roof buildings would most likely to fail when they are located near the outer boundary of the tornado core (i.e., $R/R_O \approx 1.0$), where the wind reaches its maximum speed.

Figure 10 shows the pressure distributions around the gable-roof building model as it was placed inside and outside of the tornado-like vortex core. Holmes (1993) reported a symmetric pattern for the surface pressure distribution on the surfaces of a gable-roof building model as it was placed in a straight-line wind. The pressure coefficient distributions given in Fig. 10 revealed clearly that the pressure distributions on the surfaces of the gable-roofed building model would become much more complicated when placed in a tornado-like wind. The surface pressure distributions around the gable-roof building model are not symmetric about the central plane ($Z = 0$ cross plane) of the gable-roof building model due to the swirling motion of the approaching tornado-like wind. The surface pressures on the front wall and the windward roof were found to be much higher than its counterpart at the leeward side, which results in an aerodynamic force to push the test model along the X-direction, as revealed for the force measurements shown in Fig. 9. The lower pressures on the leeward roof and walls were due to the occurrence of the large-scale flow separations in those areas, which can be seen clearly in the PIV measurements shown in Fig. 11. It can also be seen that the surface pressure on the outer side of the walls and roof (i.e., farther away from the tornado-like vortex core) were found to be higher compared with those on the inward side (i.e., closer to the tornado-like vortex center). The unbalanced pressure distributions between the inward side and the outer side of the walls and roofs would result in a net aerodynamic force to pull the building model toward the core of the tornado-like vortex, which is also confirmed from the force measurements. In addition, all the measured surface pressure values on the roof were found to be negative. Such distributions were consistent with the well-known fact that a significant low pressure would exist near the core of a tornado-like vortex, as shown quantitatively in Fig. 7.

In contrast to the findings by Holmes (1993), the pressure coefficients near the stagnation point on the front wall of a building model were not positive, as it would have been placed in a straight-line flow. As shown clearly in Fig. 10a, when the gable-roof model was placed inside the core of the tornado-like vortex (i.e., $R/R_O \approx 0.5$), a maximum surface pressure coefficient value of $-1.6$ was found on the front wall of the gable-roof building model, where the incoming air streams would impinge onto the front wall directly. It is due to the existence of the significant low pressure in the core region of a tornado-like vortex as shown in Fig. 7. A minimum pressure coefficient value of $-4.2$ was found on the leeward roof due to the flow separation on the roof, as revealed in the PIV measurement results given in Fig. 11. The negative pressure coefficients around the gable-roof building model would result in a significant uplift force (i.e., the force along Z-direction) acting on the building model, which was also confirmed from the wind load measurements given in Fig. 9.

As shown in Fig. 7, the low pressure inside the vortex core would recover gradually as the distance from the center of the tornado-like vortex increases. Therefore, when the gable-roof building model was mounted outside the tornado-like vortex core (e. g., at $R/R_O \approx 1.5$), the

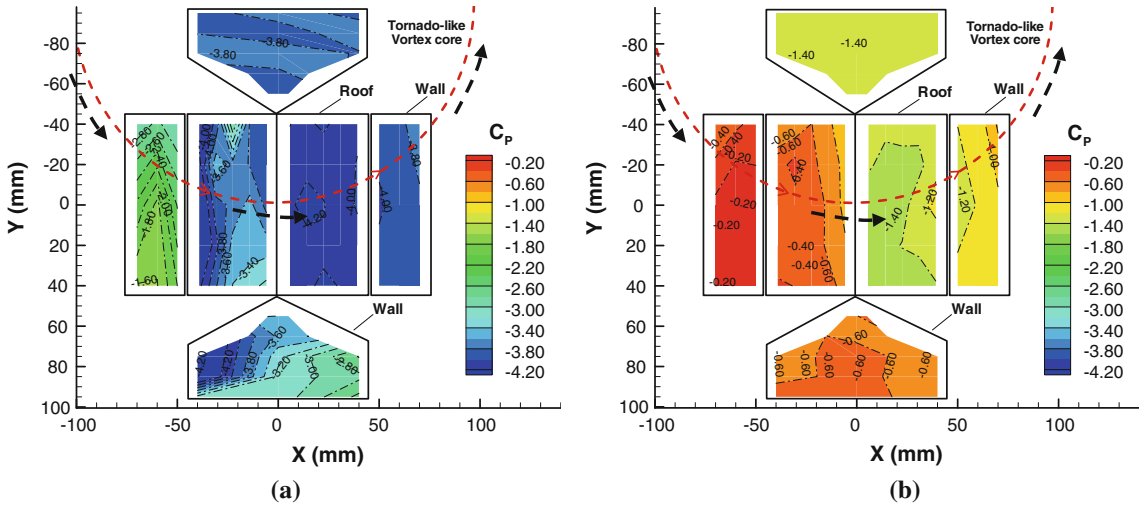


**Fig. 10** Measured pressure distributions around the gable-roof building model in tornado-like wind. **a** $R/R_O \approx 0.50$. **b** $R/R_0 \approx 1.50$

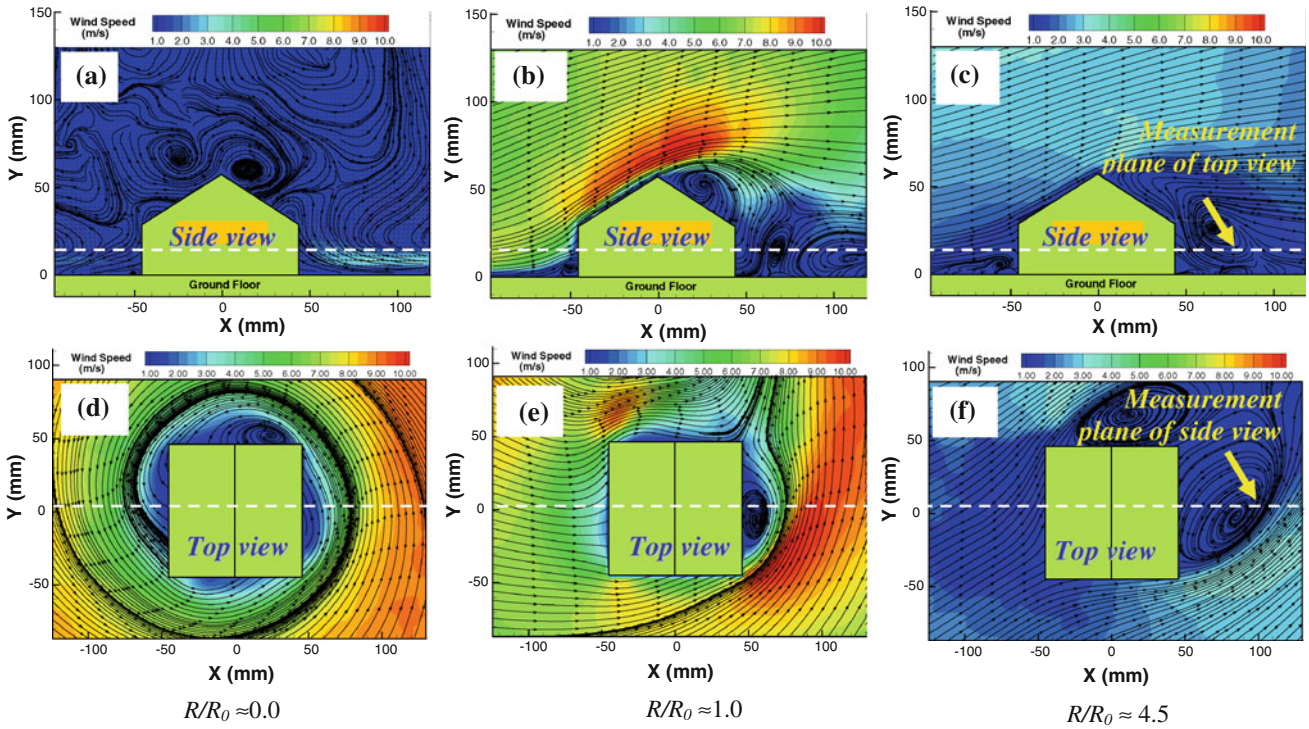


**Fig. 11** Flow structures around the gable-roofed building model in tornado-like winds. **a**, **b,** and **c** for side views; **d**, **e,** and **f** for top views

pressure coefficients on the surfaces of the test model were found to increase significantly at all the corresponding positions compared with those for the case with the building model mounted inside the vortex core at $R/R_O \approx 0.5$. As shown clearly in Fig. 10b, the peak pressure coefficient value on the front wall was found to increase to about -0.2. The minimum pressure coefficient values on the leeward roof and back wall were found to increase to about $-1.4$. As a result, the uplift force acting on the gable-roof building model would become much smaller, which was also confirmed from the wind load measurements given in Fig. 9.

With the findings derived from the wind load measurements in mind, PIV measurements were conducted to quantify the behavior of the flow structures around the gable-roof building model to elucidate underlying physics to improve our understanding about the dynamics of the flow-structure interactions between the test building model and tornado-like winds. Figure 11 shows both the side and top views of the flow structures around the gable-roofed

building model as the test model was mounted at the center of the vortex core (i.e., $R/R_O \approx 0.0$ for Fig. 11a, d), at the boundary between the inner core and outer region where local wind speed reaches maximum (i.e., $R/R_O \approx 1.0$ for Fig. 11b, e), and at the outer region far away from the center of the tornado-like vortex (i.e., $R/R_O \approx 4.5$ for Fig. 11c, f), respectively. Yang (2009) conducted an experimental study to reveal the characteristics of the flow structures around the same gable-roof building model in a straight-line, atmospheric boundary wind. Some typical ensemble-averaged PIV measurement results of the flow field around the same gable-roof building model in a straight-line, atmospheric boundary wind are shown in Fig. 12 for comparison.

It can be seen clearly that, compared with those in straight-line winds shown in Fig. 12, the wake vortices and flow structures around the gable-roof building model in tornado-like winds were found to become much more complicated. When the gable-roof building model was mounted near the center of tornado-like vortex (i.e., $R/R_O \approx 0$), as shown clearly in Fig. 11a, two large vortices were found to form above the roof of the building model when the downdraft jet in the vortex core met with the air streams from outer region. While the wind speed is relatively low inside the vortex core, it can still be seen clearly that the air streams in the other region near the ground would move toward the test model and turn upward abruptly before reaching the side walls of the test building model. As shown clearly in Fig. 11d, the top view of the flow field reveals an almost axisymmetric flow pattern around the building model. The streamlines farther away from test model were found to be in a spiral flow pattern, as expected. Since the local wind speed in the tornado-like vortex core was relatively low, except for the uplift force caused mainly by the significant low pressure in the tornado-like vortex core, the other two components of the aerodynamic force acting on the gable-roof building model would be relatively small as the model was mounted near the center of the tornado-like vortex, which was confirmed from the wind load measurements shown in Fig. 9.

Figure 11b, e show the side and top views of the flow field around the gable-roof building model when the test model was mounted near the outer boundary of the tornado-like vortex core (i.e., $R/R_O \approx 1.0$). As described above, this is the position where maximum wind speed was observed. The significant wind loads were also found at this location according to the wind load measurements. The ensemble-averaged PIV measurement result in the vertical plane (i.e., side view) reveals clearly that, while a region with higher wind speed was formed above the windward roof of the test model, a large recirculation bubble was found to sit on the leeward roof. The flow separation would cause in low pressure region on the leeward roof as revealed from the pressure measurements. In addition, two recirculation bubbles were also found to be generated in the wake near the ground when the test model was mounted in tornado-like winds. For comparison, as shown clearly in Fig. 12a, only one large recirculation bubble was found in the wake when the same gable-roof building model was placed in a straight-line, atmospheric boundary layer wind.

As expected, as the test model was placed in a straight-line atmospheric boundary layer wind, the top view of PIV measurement results (i.e., see Fig. 12b) reveals that the streamlines around the gable-roof building model would be symmetrical to the center plane of the test model. Two symmetrical circulation bubbles were formed in the wake of the building model. It should be noted that the two symmetrical circulation bubbles were actually the sectional

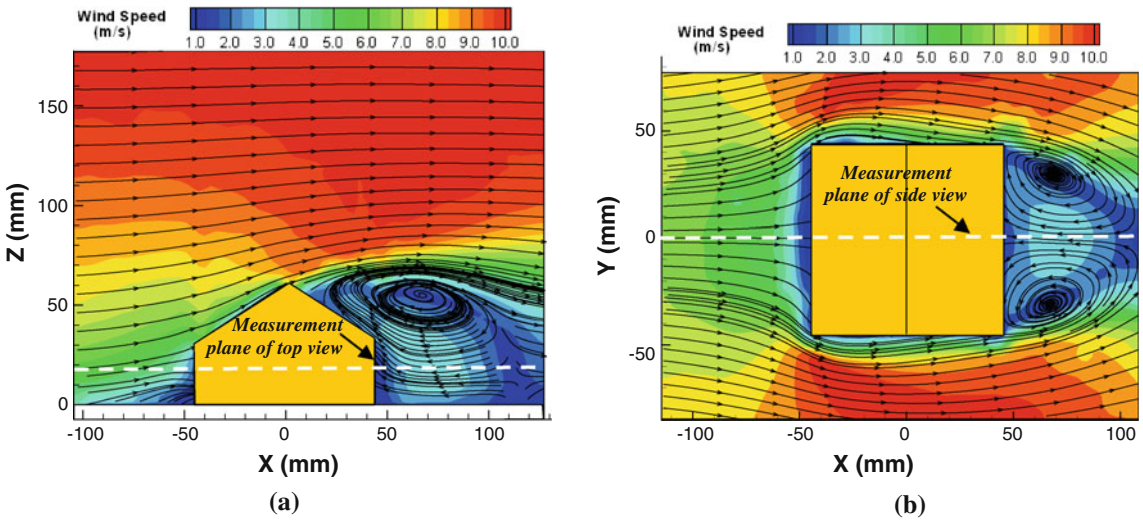


**Fig. 12** Flow structures around the gable-roofed building model in a straight-line, atmospheric boundary layer wind. **a** Side view. **b** Top view

view of the two legs of a complicated 3D wake vortex formed at the downstream of the test model. However, as the same gable-roof building model mounted in a swirling, tornado-like wind, the streamlines around the test model in the horizontal plane were found to become much more interesting and complicated, as shown clearly in Fig. 11e. Due to the lower pressure in the core of the tornado-like vortex, the incoming air streams, which were almost perpendicular to the front wall of the test model, were found to turn rapidly toward the core of the tornado-like vortex after passing the test model. As a result, instead of forming two symmetrical circulation bubbles in the wake of the building model as those in the straight-line wind, only one much smaller circulation bubble was found to form near the outer corner of the leeward wall of the test model.

Figure 11c, f shows the side and top views of the PIV measurements of the flow fields around the test model as the gable-roof building model was mounted in the outer region far away from the core of the tornado-like vortex (i.e., at the location of $R/R_O \approx 4.5$). As described above and visualized clearly in Fig. 5d, the flow field would have significant radial velocity components ($V_R$) in the outer region, and the streamlines were found to be almost parallel lines tilting toward the vortex core near $R/R_O \approx 4.5$. It was revealed clearly that the flow features around the gable-roof building model at this location would become quite different from the cases with the test model mounted inside or at the boundary of the tornado-like vortex core. The air streams were found to separate more readily from the corners of the test model as they approaching of the gable-roof building model. As a result, a large recirculation bubble was found to be formed above the leeward roof and downstream of the back wall of the test model in the side view given in Fig. 11c. Since the incoming streamlines in the top view given in Fig. 11f were almost parallel lines tilting toward the vortex core, the air streams just like those in a straight-line wind to approach the test model with an orientation angle. As a result, two large recirculation bubbles were found in the top view at the downstream of the leeward wall and inner side wall of the test model. As shown clearly in Fig. 6, as the distance from center of the tornado-like vortex increases, the local wind speed would become smaller and smaller in the outer region, and the low pressure will also be recovered eventually. Therefore, the aerodynamic forces and resultant moments acting on the test model would decrease gradually with the increasing distance, which were confirmed quantitatively from the wind load measurements shown in Fig. 9.

### 3.2.2 *The effects of the orientation angle of the test model in tornado-like winds*

In the present study, the effects of the orientation angle of the test building model related to the tornado-like vortex on the characteristics of the wake vortices and flow structures around the test model as well as the resultant wind loads (forces and moments) acting on the test model were also investigated. Figure 13 shows the measured three components of the aerodynamic force acting on the test model as functions of the orientation angle when the test model was mounted in the tornado-like wind at the location of $R/R_O \approx 1.0$ [i.e., the profiles of $CF_X(T)$, $CF_Y(T)$ and $CF_Z(T)$]. The measured aerodynamic force coefficients of the same gable-roof building model in a straight-line, atmospheric boundary layer wind with the same maximum wind speed of 10 m/s at the eave height of the building model [i.e., $CF_X(S)$, $CF_Y(S)$, and $CF_Z(S)$] were also plotted in the graph for quantitative comparison. It can be seen clearly that, for the same gable-roof building model, the force coefficients were found to become much bigger in tornado-like winds than those in the straight-line wind at all the compared orientation angles. More specifically, the magnitude of the resultant aerodynamic force acting on the gable-roof building model in tornado-like wind would be about 3–4 times higher than that in the straight-line wind with the same orientation angle. The result was found to agree with the findings of Jischke and Light (1983) and Bienkiewicz and Dudhia (1993) well. It can also be seen that, as the gable-roof building model was mounted in the tornado-like winds, the uplift force (i.e., Z-component) was found to be always much bigger than the other two components, which is mainly due to the significant low pressure near the core region of the tornado-like vortex. While the maximum value of the uplift force was found at the orientation angle of OA ≈ 15.0–30.0 degrees, the streamwise pushing force acting on the building model (i.e., X-component) was found to reach its maximum value at OA ≈ 45.0 degrees, which might be due to the maximum projected area (i.e., blockage) along the incoming flow direction. While the Y-component of the aerodynamic

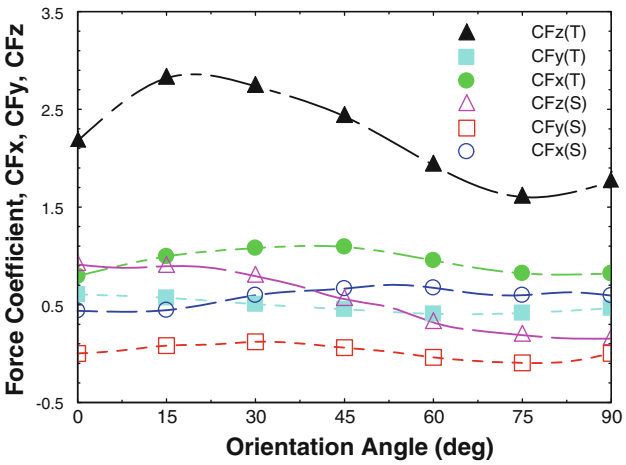


**Fig. 13** The measured force coefficients versus the orientation angle

force was found to be always the smallest among the three components of the aerodynamic force, its magnitude is almost independent to the orientation angle in tornado-like winds. It should also be noted that, when the test model was placed in the straight-line wind, the lateral component (i.e., Y-component) of the aerodynamic force acting on the test model would change its sign at OA $\approx$ 45.0 degrees. However, the Y-component of the force coefficients was found to be positive at all the orientation angles as the test model was mounted in tornado-like winds, which indicates that the building model would always be pushed toward to the center of the tornado-like vortex. Figure 14 shows the

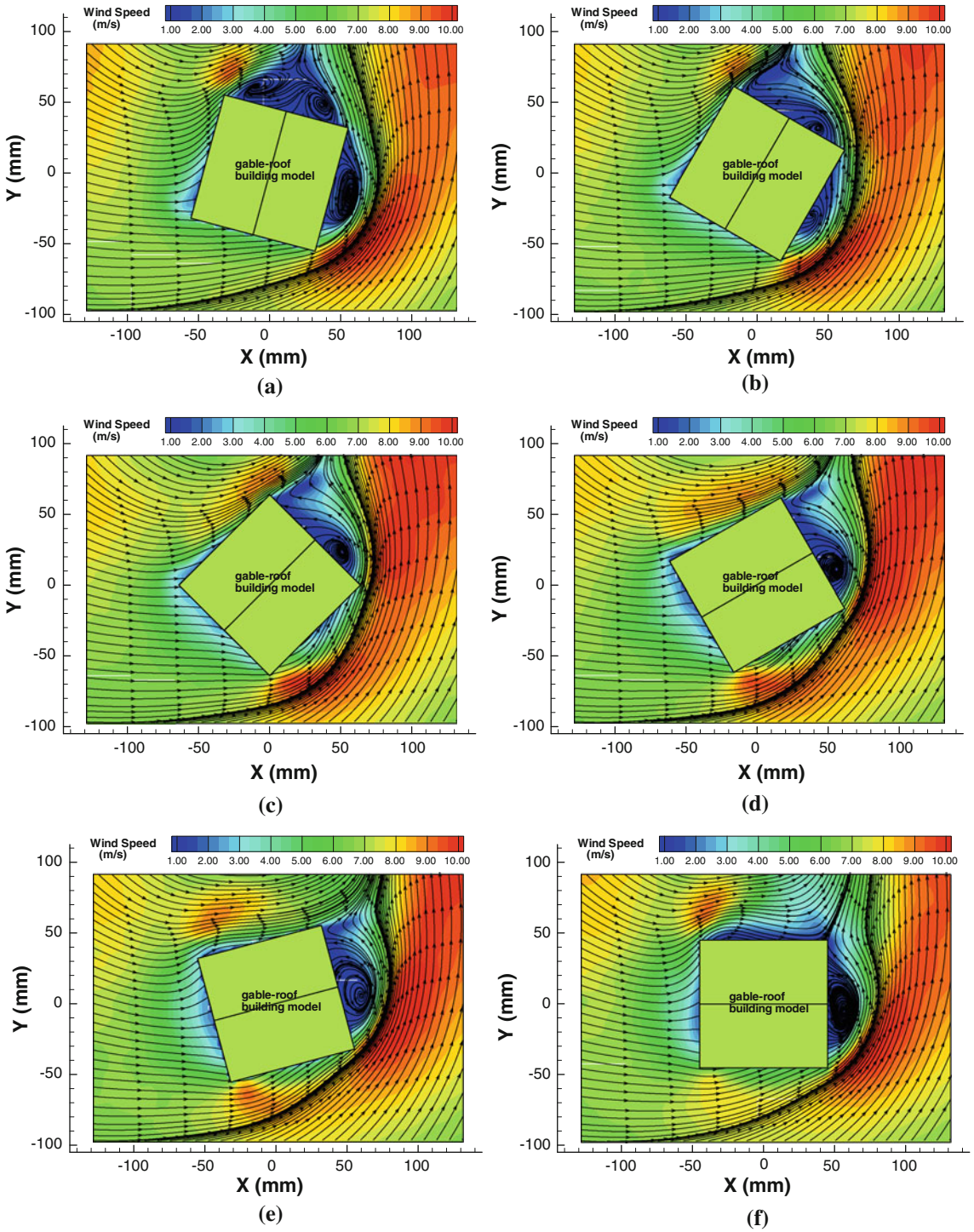


**Fig. 14** Flow field around the test model vs. the orientation angles in the $Z/R_O \approx 0.10$ horizontal plane. **a** OA = 15 deg. **b** OA = 30 deg. **c** OA = 45 deg. **d** OA = 60 deg. **e** OA = 75 deg. **f** OA = 90 deg

ensemble-averaged PIV measurement results in the horizontal plane of $Z/R_O \approx 0.10$ (i.e., crossing the half eave height of the gable-roof building model) with the test model mounted in tornado-like winds at $R/R_O \approx 1.0$ with different orientation angles. The variations of the wake vortices and flow structures around the gable-roof building model with the orientation angle of the test model related to the tornado-like vortex were elucidated clearly from the PIV measurement results.

Based on the PIV measurements in horizontal planes at different elevations as well as in different vertical planes parallel to the side walls of the test model, the 3-D flow velocity fields around the gable-roof building model in tornado-like winds were reconstructed. Figure 15a shows one example of the reconstructed 3-D flow fields around the gable-roof building model with the test model mounted at $R/R_O \approx 1.0$ and $OA = 0.0$ deg. The 3-D vortex structures in the wake of the gable-roof building model in the tornado-like wind can be extracted from the reconstructed 3-D flow velocity fields. Figure 15b, c shows the perspective views of the reconstructed 3-D wake vortex structures in the wake of the gable-roofed building model in the term of iso-surfaces of the local vorticity. The 3-D features of the complex vortex and flow structures in the wake of the gable-roofed building model in tornado-like winds were visualized clearly from the reconstructed 3-D flow fields.

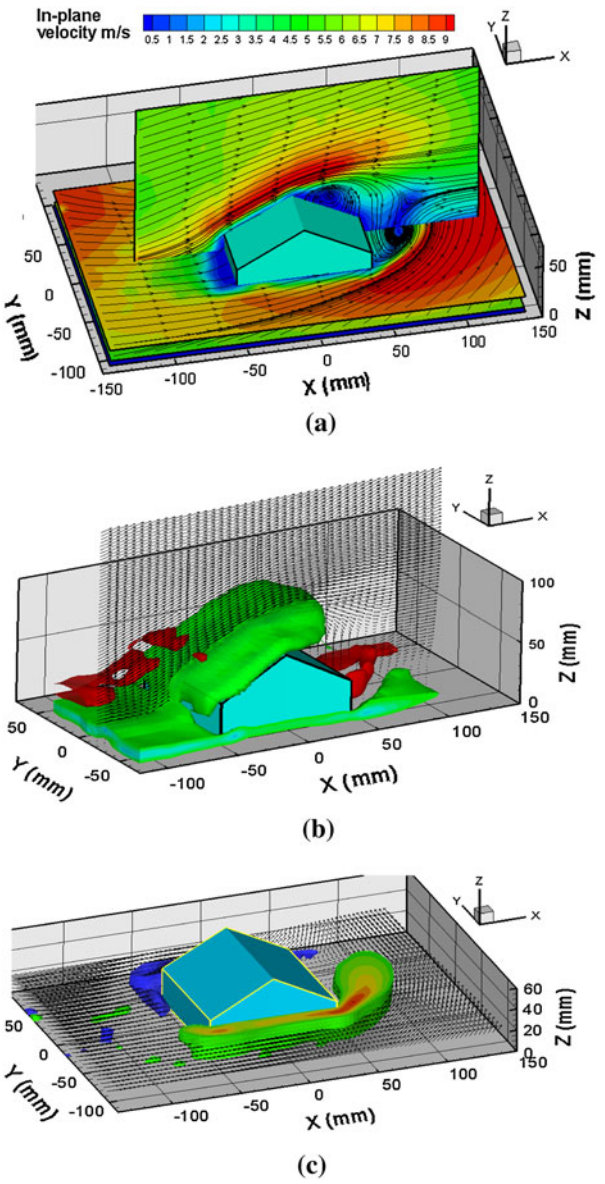


**Fig. 15** The prospective views of the reconstructed 3-D flow field and iso-surfaces of the vorticity field around the gable-roof building model in a tornado-like wind. **a** The reconstructed 3-D flow field. **b** Iso-surfaces of the Y-component of the vorticity vectors. **c** Iso-surfaces of the Y-component of the vorticity field

## 4 Conclusions

An experimental study was conducted to quantify the characteristics of a tornado-like vortex and to reveal the dynamics of the flow-structure interactions between a low-rise, gable-roof building model and swirling tornado-like winds. In addition to measuring wind loads (i.e., aerodynamic forces and moments) and pressure distributions on the surfaces of the test model, a digital Particle Image Velocimetry (PIV) system was used to conduct detailed flow field measurements to quantify the wake vortex and turbulent flow structures around the gable-roof building model in tornado-like winds. The effects of important parameters, such as the distance between the centers of the tornado-like vortex and the test model and the orientation angles of the building model related to the tornado-like vortex, on the wake vortices and flow structures around the gable-roof building model as well as the wind loads induced by the tornado-like vortex were assessed quantitatively.

The PIV measurement results reveal clearly that a tornado-like vortex is a very complex three-dimensional vortex flow. While the instantaneous PIV measurement results reveal clearly that the tornado-like vortex was highly turbulent with its center wandering around randomly, a well-defined flow pattern can be identified clearly from the time-averaged PIV measurement results. In addition to a strong upward flow in the outer region and downdraft jet flow in the vortex core in the vertical direction, an axisymmetric flow pattern in the form of a well-defined vortex structure can be seen clearly in the horizontal planes. The ensemble-averaged flow field of the tornado-like vortex in each horizontal plane could be divided into two regions: an inner core region and an outer region. In the inner core region, air streams were found to

flow concentrically with the wind speed increasing linearly with the increasing radial distance away from the center of the vortex. Wind speed was found to reach its maximum value at the outer boundary of the tornado-like vortex core and then begins to decrease with the increasing distance from the center of the vortex core in the outer region. The flow velocity vectors in the outer region were found to have significant radial components, which results in a strong spiral motion that sucks surrounding air flowing toward the vortex core.

The wind loads (both force and moments) acting on the test gable-roof building model induced by tornado-like wind were found to vary significantly with the position of the test model in relation to the center of the tornado-like vortex. Due to the significant low pressure in the core of the tornado-like vortex, the test model was found to experience a significant uplift force to try to lift the test model off the ground as the test model was mounted inside the vortex core. Corresponding to the maximum local wind speed, the tangential and radial components of the aerodynamic force acting on the test model were found to reach their maximum values when the test model was mounted on the boundary of the tornado-like vortex core. Unlike those in straight-line winds, the wake vortex and flow structures around the test model in tornado-like winds were found to become quite unsymmetrical and much complicated. The orientation angle of the test model related to the tornado-like vortex was found to have considerable effects on the wake flow pattern around the test model as well as the resultant wind loads acting on the building model. The uplift force acting on the gable-roof building model, which is the most dominant force induced by the tornado-like vortex, was found to reach its maximum value at the orientation angle of OA $\approx$ 15–30 degrees. The wind loads acting on the gable-roof building model in tornado-like winds were found to be at least 3 times higher compared with those in a straight-line, atmospheric boundary layer wind at all the compared orientation angles.

**Acknowledgments** This research was funded by National Oceanic and Atmospheric Administration (NOAA)-Award # NA060AR4600230 with Mr. John Gaynor as the program manager. The authors also want to thank Mr. Bill Richard of Iowa State University for his help in manufacturing the test models.

## References

Bienkiewicz B, Dudhia P (1993) Physical modeling of tornado-like flow and tornado effects on building loading. In: Proceeding 7th US National Conference on Wind Engineering, pp 95–106

Bluestein HB, Golden JH (1993) A review of tornado observations. The Tornado: its structure, dynamics, prediction and hazards. Geophys. Monogr., No. 79, American Geophysics Union, pp 19–39

Brooks HE, Doswell CA III (2001) Normalized damage from major tornadoes in the United States: 1890–1999. Weather Forecast 16(1):168–176

Castro IP, Robins AG (1977) The flow around a surface-mounted cube in uniform and turbulent streams. J Fluid Mech 79:307–335

Cermak JE (1975) Applications of fluid mechanics to wind engineering—a Freeman Scholar lecture. J Fluids Eng 97:9–38

Chang CC (1971) Tornado effects on buildings and structures with laboratory simulation. In: Proceedings of 3rd International Conference on Wind Effects on Buildings and Structures, Tokyo, Japan, pp 151–174

Church CR, Snow JT, Agee EM (1977) Tornado vortex simulation at Purdue University. Bull Am Meteorol Soc 58:900–908

Davies-Jones RP (1976) Laboratory simulations of tornadoes. In: Proceedings, Symposium on Tornadoes, Texas Tech University, pp 51–174

Doswell CA III, Edwards R, Thompson RL, Hart JA, Crosbie KC (2006) A simple and flexible method for ranking severe weather events. Weather Forecast 21(6):939–951

Forbes G (2006) Meteorological aspects of high-impact tornado outbreaks. In: Proceedings of Extended Abstracts, Symposium on the Challenges of Severe Convective Storms (CD-ROM), AMS, Atlanta, pp 1–12

Grazulis TP (1993) Significant tornadoes: 1680–1991, The Tornado Project, St. Johnsbury, Vt., 1326

Haan FL, Sarkar PP, Gallus WA (2008) Design, construction and performance of a large tornado simulator for wind engineering applications. Eng Struct 30:1146–1159

Haan FL, Balaramudu VK, Sarkar PP (2010) Tornado-induced wind loads on a low-rise building. J Struct Eng 136:106–116

Holmes JD (1993) Wind load on low-rise building—a review. CSIRO, Division of Building Research, Highett

Hunt JCR, Abell CJ, Peterka JA, Woo H (1978) Kinematical studies of the flows around free or surface-mounted obstacles: applying topology to flow visualization. J Fluid Mech 86(1):179–200

Jischke MC, Light BD (1983) Laboratory simulation of tornadic wind loads on a rectangular model structure. J Wind Eng Ind Aerodyn 13:371–382

Kanda M, Maruta E (1993) Characteristics of fluctuating wind pressure on long low-rise buildings with gable roofs. J Wind Eng Ind Aerodyn 50:173–182

Kim KC, Ji HS, Seong SH (2003) Flow structure around a 3-D rectangular prism in a turbulent boundary layer. J Wind Eng Ind Aerodyn 91:653–669

Krajnovic S, Davidson L (1999) Large-eddy simulation of the flow around a surface-mounted cube using a dynamic one-equation subgrid model. In: Banerjee S, Eaton J (ed) First International Symposium on Turbulence and Shear Flow Phenomena, Begel House, Inc, New York

Lee BD, Wilhelmson RB (1997a) The numerical simulation of non-supercell tornadogenesis. Part I. Initiation and evolution of pretornadic misocyclone circulation along a dry outflow boundary. J Atmos Sci 54:32–60

Lee BD, Wilhelmson R (1997b) The numerical simulation of non-supercell tornadogenesis. Part II. Evolution of a family of tornadoes along a weak outflow boundary. J Atmos Sci 54:2387–2415

Liu Z, Prevatt DO, Aponte-Bermudez LD, Gurley K, Reinhold T, Akins RE (2009) Field measurement and wind tunnel simulation of hurricane wind loads on a single family dwelling. Eng Struct 31(10):2265–2274

Markowski PM, Straka J, Rasmussen EN (2002) Direct surface thermodynamic observations within the rear-flank downdrafts of nontornadic and tornadic supercells. Mon Weather Rev 130:1692–1721

Martinuzzi R, Tropea C (1993) The flow around surface-mounted, prismatic obstacles placed in a fully developed channel flow. J Fluids Eng 115:85–92

Mishra AR, James DL, Letchford CW (2008a) Physical simulation of a single-celled tornado-like vortex, part A: flow field characterization. J Wind Eng Ind Aerodyn 96:1243–1257

Mishra AR, James DL, Letchford CW (2008b) Physical simulation of a single-celled tornado-like vortex, Part B: Wind loading on a cubical model. Journal of Wind Engineering and Industrial Aerodynamics 96:1258–1273

Natarajan D (2011) Numerical simulation of tornado-like vortices. PhD thesis, Department of Civil and Environmental Engineering, the University of Western Ontario

Nolan DS, Farrell BF (1999) The structure and dynamics of tornado-like vortices. J Atmos Sci 56:2908–2936

Peterka JA, Hosoya N, Dodge S, Cochran L, Cermak JE (1998) Area average peak pressures in a gable roof vortex region. J Wind Eng Ind Aerodyn 77–78(1):205–215

Samaras T (2008) Private communication

Schecter DA, Nicholls ME, Persing J, Bedard AJJ, Pielke RAS (2008) Infrasound emitted by tornado-like vortices: basic theory and a numerical comparison to the acoustic radiation of a single-cell thunderstorm. J Atmos Sci 65:685–713

Sengupta A, Haan FL, Sarkar PP, Balaramudu V (2008) Transient loads on buildings in microburst and tornado winds. J Wind Eng Ind Aerodyn 96:2173–2187

Shah KB, Ferziger JH (1997) A fluid mechanicians view of wind engineering: large eddy simulation of flow past a cubic obstacle. Journal of Wind Engineering and Industrial Aerodynamics 67(68):211–224

Sousa JMM (2002) Turbulent flow around a surface-mounted obstacle using 2D–3C DPIV. Exp Fluids 33:854–862

Sousa JMM, Pereira JCF (2004) DPIV study of the effect of a gable roof on the flow structure around a surface-mounted cubic obstacle. Exp Fluids 37:409–418

Speheger DA, Doswell CA III, Stumpf GJ (2002) The tornadoes of 3 May 1999: Event verification in central Oklahoma and related issues. Weather Forecast 17(3):362–381

Stathopoulos T, Wank K, Wu H (2001) Wind pressure provisions for gable roofs of intermediate roof slope. Wind Struct 4:119–130

Uematsu Y, Iizumib E, Stathopoulos T (2007) Wind force coefficients for designing free-standing canopy roofs. J Wind Eng Ind Aerodyn 95:1486–1510

Ward NB (1972) The exploration of certain features of tornado dynamics using a laboratory model. J Atmos Sci 29:1194–1204

Womble JA, Smith DA, Mehta KC, McDonald JR (2009) The enhanced Fujita scale: for use beyond tornadoes? Forensic Engineering 2009: Pathology of the Built Environment Proceedings of the Fifth Congress on Forensic Engineering

Wurman J, Alexander CR (2005) The 30 May 1998 Spencer, South Dakota, Storm. Part II: comparison of observed damage and radar-derived winds in the tornadoes. AMES Mon Weather Rev 133:97–118

Wurman J, Gill S (2000) Finescale radar observations of the Dimmitt, Texas (2 June 1995), tornado. AMS Mon Week Rev 128:2135–2164

Yakhot A, Anor T, Liu H, Nikitin N (2006) Direct numerical simulation of turbulent flow around a wall-mounted cube: spatio-temporal evolution of large-scale vortices. J Fluid Mech 566:1–9

Yang Z (2009) Experimental investigations on complex vortex flows using advanced flow diagnostic techniques. PhD thesis, Department of Aerospace Engineering, Iowa State University

Yang Z, Sarkar P, Hu H (2010) Visualization of flow structures around a gable-roofed building model in tornado-like winds. J Vis 13(4):285–288

Yang Z, Sarkar P, Hu H (2011) An experimental study of a high-rise building model in tornado-like winds. J Fluids Struct. doi: 10.1016/j.jfluidstructs.2011.02.011